GEOPHYSICAL RESEARCH LETTERS, VOL. 24, NO. 22, PAGES 2737-2740, NOVEMBER 15, 1997

Rate parameter uncertainty effects in assessing stratospheric ozone depletion by supersonic aviation

Manvendra K. Dubey, Gregory P. Smith, and W. Seth Hartley

Molecular Physics Laboratory, SRI International, Menlo Park CA

Douglas E. Kinnison and Peter S. Connell

Lawrence Livermore National Laboratory, Livermore CA

Abstract. Box model sensitivity-uncertainty calculations for O_3 depletion from supersonic aircraft emissions were performed at the most perturbed locale using localized outputs of the LLNL 2-D diurnally averaged assessment model. Processes controlling N_2O_5, catalytic O_3 loss steps $O+NO_2$ and HO_2+O_3, HOx sink reactions $OH+ HNO_3/HNO_4$, and the $O+O_2$ recombination that forms O_3 are identified as the dominant photochemical uncertainty sources. Guided by local sensitivities, 2-D model runs were repeated with 9 targeted input paramcters altered to 1/3 of their 1-σ uncertainties to put error-bounds on the predicted O_3 change. Results indicate these kinetic errors can cause the predicted local O_3 loss of 1.5% to be uncertain by up to 3% in regions of large aircraft NOx injection.

Introduction

Proposals to build a fleet of high speed civil transports (HCSTs) have stimulated new research on effects of aircraft emissions on stratospheric O_3(Stolarski et al., 1995). Renewed interest derives from economic growth in the aircraft industry, now accounting for 3% of global fossil fuel consumption(WMO, 1994); technological advances promising lower NOx emissions in the lower stratosphere where O_3 destruction is a concern; and advances in stratospheric chemistry knowledge since the problem was first outlined by Johnston(1971). Mechanism improvements, including interactions with chlorine compounds and aerosols, suggest less O_3 destruction from NOx emissions(Stolarski et al., 1995).

Current assessments of O_3 change by HSCTs rely on the accuracy of comparative 2-D model runs. Consensus results from 5 modelers(Stolarski et al., 1995) suggest a fleet of 500 HSCTs flying at Mach 2.4 (18-20km) with an emission index of 15g(NO_2)/kg fuel in 2015 (Cly levels of 3 ppb) would reduce global O_3 by about 0.5-1%, with 1-2% reductions at high latitudes. The models differ, notably in their treatments of transport, and the 0.5% variation in the predicted HSCT effects on global O_3 provides some indication of the assessment uncertainty from possible errors. Observations used for model validation should narrow this gap.

Photolysis and kinetics rate parameters in these 2-D models are from the NASA-JPL evaluation(DeMore et al., 1994), which also includes error limits that will propagate into the uncertainty in the assessment. We recently applied a box model sensitivity code, Senkin(Lutz et al., 1988), to a survey of selected locations in the LLNL 2-D atmospheric model(Wuebbles et al., 1993) to quantify the specific reaction rates controlling local O_3 concentrations. Sensitivity coefficients $S_i(O_3) = \partial[O_3]/[O_3] / (\partial k_i/k_i)$ (relative O_3 change for a fractional rate constant change) can also be used to propagate rate constant uncertainties (δk_i) into a model uncertainty in the predicted concentration. We apply this approach here to systematically examine and quantify the uncertainties in predicted HSCT effects on O_3 levels due to possible errors in all the input photochemical parameters. We focus here as a representative choice on one scenario and 4 altitudes at 47°N in June, where maximum NOx emissions are introduced and persist due to slow mixing. Local sensitivity-uncertainty analysis is used to identify the reactions that dominate the uncertainty. These key input rate parameters are altered and 2-D computations are repeated to estimate error limits for the predicted O_3 change. These results are compared with the uncertainty estimated by the box model sensitivity approach.

Computational Approach

We have conducted a localized sensitivity-uncertainty analysis on two scenarios modeled by the 2-D diurnally-averaged, seasonally-varying LLNL chemical-radiative-transport atmospheric model. The photochemical mechanism has 47 photolyses, 107 reactions including hydrolysis of N_2O_5 and $ClONO_2$ on aerosols, and no family approximations. The Senkin box model sensitivity code was applied with exactly the same kinetics to localized outputs of this model at 47°N in June 2015 at altitudes of 17.25, 20.25, 21.75, and 26.25km for 2 scenarios(Stolarski et al., 1995): the reference background subsonic fleet scenario(called SCN0 here), and SCN4, which simulates the net emissions from the HSCT fleet described above.

Senkin(Lutz et al., 1988) efficiently computes all species concentration derivatives with respect to the input rate parameters in the process of solving the kinetics rate equations, to provide local linear sensitivity coefficients $S_i(O_3) = \partial(\ln[O_3])/\partial\ln k_i$ for 0-D problems. A local fractional change or uncertainty in a species abundance is predicted by the product of the fractional change in rate constant and the appropriate normalized sensitivity coefficient: $U_i(X)/[X] = S_i(X)\ \delta k_i/k_i$, and the total expected kinetic error in model species concentration for a given box is estimated by taking the square root of the sum of the squares. (The temperature dependent DeMore et al.[1994] error functions imply Gaussian distributions.) The sensitivity coefficient of the ratio of O_3 between two scenarios is simply the difference of the respective logarithmic sensitivity coefficients. So differences between the perturbed SCN4 (*) and standard SCN0 O_3 sensitivity coefficients iden-

Paper number 97GL02859.
0094-8534/97/97GL-02859$05.00

tify those steps that must be well known for accurate assessments: $S_i'(\Delta O3) = S_i(O_3*/O_3) = S_i(O_3*) - S_i(O_3)$. Combining the Senkin $S_i'(\Delta O_3)$ with the temperature dependent NASA-JPL 1-σ rate constant error-bars at 220K, we derive uncertainty estimates for predicted HSCT effects on O_3 at these locales. The boxes chosen for examination were selected to uncover significant sensitivity, and the choice of the NASA error-bars represents a broad estimate of possible kinetic uncertainty.

Because sensitivity coefficients represent the time-dependent propagation of an infinitesimal rate parameter perturbation, individual sensitivities grow and converge on the local photochemical timescale. Each box's June kinetics were integrated for 2-3 years to get converged sensitivities. During this time we need the 0-D species concentrations to remain at the local instantaneous solution of the original June 2-D model box. In our procedure, instantaneous local production minus loss(P-L) rates were taken from the LLNL 2-D model output for each species in each run. These P-L terms describe how much a concentration deviates from local photostationary state due to all fluxes from other locations and times, and reflect effects of transport and previous seasons. When we include these same P-L terms (divided by 2-D model concentration) as fixed first order rate constants in the mechanism, we do maintain our box model at the steady June 2-D model solution, while integrating the sensitivities to convergence.

However, we find that the large radical species P-L terms have high sensitivities which damp the sensitivities to the photochemical terms. We add all the P-L terms within a particular family in order to obtain a much smaller net P-L term, due to cancellations. This eliminates the damping, but still keeps the solution stable and locked at the LLNL result during computation. In this study, for each individual box, the net family P-L terms were added and assigned (with no iteration) to the family member with the largest flux in the same direction: NO, Cl, Br, and H_2O_2. Long-lived trace gases H_2O, CH_4, N_2O, and CFC's were kept constant. An effective O_3 P-L term is also used to freeze this concentration at its June values. We computed small sensitivities to the above P-L terms, and they largely cancel out when evaluating the difference sensitivity to the HSCT perturbation. Their small magnitude ($\leq$0.02 for O_3 and NO) further implies that this procedure does not damp out any significant sensitivities to long timescale processes.

0-D Sensitivity Analysis Results

Table 1 lists the 0-D sensitivities and uncertainties for the most significant reactions at 4 altitudes for 47°N in June. As the first two columns show, the HSCT O_3 perturbation sensitivity(2) differs considerably from that for O_3(1) - many NOx reactions are more prominent, with little remaining sensitivity to O_2 or O_3 photolysis or the OH and NO+O_3 reactions. The last four columns(4-7) list the uncertainty in HSCT O_3 perturbation for each reaction and altitude, the product of the 1-σ rate constant uncertainty(3) and $S'(\Delta O_3)$. This analysis predicts the size and sign of the effect of varying the rate constants to their JPL 1-σ limits on the local HSCT-induced O_3 depletion; for example at 20 km, a 27% increase in the O+NO_2 rate constant gives an additional O_3 depletion of 3.1%, while a 87% decrease in the HO_2+O_3 rate constant exacerbates O_3 losses by 2.6%. The table reveals that 10 reactions contribute most(85-90%) of the assessment prediction uncertainty. These uncertainty factors are plotted with their signs in Fig. 1.

N_2O_5 reactions are prominent in Fig. 1 because it is the largest HSCT chemical perturbation (up 80% at 20km), and the kinetics controlling its abundance have large error limits(50-100%). A mirror image pattern appears for competing reaction pairs that determine the active NOx/NOy fraction, such as N_2O_5 formation and heterogeneous hydrolysis that sequester NOx versus photolysis back to active NOx, and HNO_3 formation versus its photolysis. (Note the important N_2O_5 hydrolysis sensitivity can also be applied to uncertainties in aerosol loading.) The HSCT NOx injection increases catalytic O_3 loss from O+NO_2 ,which competes with O_3 formation by O+O_2, while reducing loss by HO_2+O_3. O_3 losses worsen upon

Table 1. Sensitivity Coefficients & Uncertainty Factors at 47°N. $S(O_3) = \partial(\ln[O_3])/\partial(\ln k)$; $S'(\Delta O_3) = S(O_3*)-S(O_3)$; $U' = S'(\Delta O_3)\ \delta k/k$

	1	2	3	4	5	6	7
Reaction	S(20)	S'(ΔO3)	δk/k	U'(17)	U'(20)	U'(22)	U'(26)
* O + O2	.2916	.1083	0.265	.0139	.0287	.0218	.0056
O(D) + air	.1091	-.0371	0.35	-.0090	-.0130	-.0087	-.0030
O(D) + H2O	-.0736	.0359	0.35	.0098	.0126	.0093	.0029
O(D) + N2O	-.0027	-.0177	0.47	-.0086	-.0083	-.0069	-.0012
O(D) + CH4	-.0227	.0163	0.35	.0049	.0057	.0038	.0008
OH + O3	-.1318	.0050	0.87	.0073	.0044	.0012	.0023
* HO2 + O3	-.1408	.0299	0.87	.0254	.0260	.0165	.0032
OH + HO2	. 0205	-.0155	0.66	-.0087	-.0103	-.0074	-.0029
NO + O3	-.1242	-.0093	0.53	-.0096	-.0049	-.0043	-.0024
HO2 + NO	.0837	.0119	0.32	.0028	.0038	.0029	.0013
* O + NO2	-.2177	-.1140	0.27	-.0143	-.0308	-.0244	-.0073
NO2 + O3	-.0182	.0151	0.38	.0002	.0057	.0047	.0012
HO2 + NO2	.0546	-.0312	0.32	-.0093	-.0100	-.0048	-.0014
* NO2 + NO3	-.0132	.0491	0.67	.0179	.0329	.0223	.0037
* N2O5 hydrol..	-.0112	.0328	0.50	.0086	.0164	.0110	.0011
OH + NO2	.0623	.0496	0.39	.0090	.0194	.0154	.0050
* OH + HNO3	.0539	-.0506	0.66	-.0206	-.0334	-.0233	-.0044
* OH+HNO4	.0283	-.0199	1.08	-.0207	-.0215	-.0137	-.0024
NO2 + hv	.1274	.0063	0.20	.0034	.0013	.0011	.0007
NO3+hv ->O	.0394	-.0340	1.00	-.0168	-.0340	-.0293	-.0038
NO3+hv ->O2	-.0308	-.0114	1.00	-.0111	-.0114	-.0076	-.0007
* N2O5 + hv	.0102	-.0378	1.00	-.0191	-.0378	-.0276	-.0044
* HNO3 + hv	-.0641	-.0573	0.30	-.0093	-.0172	-.0126	-.0033
HNO4 + hv	-.0191	.0109	1.00	.0107	.0109	.0107	.0012
CH2O + hv	-.0162	.0117	0.40	.0058	.0047	.0027	.0004
Cl + O3	-.0379	.0229	0.30	.0042	.0069	.0053	.0012
ClO + NO	.0318	-.0208	0.30	-.0037	-.0062	-.0047	-.0011
ClO + NO2	-.0053	.0100	0.59	.0040	.0059	.0040	.0001
OH + HCl	-.0305	.0205	0.35	.0048	.0072	.0045	.0009
BR + O3	-.0086	.0050	0.53	.0026	.0026	.0023	.0002
BRO + NO2	.0088	.0012	0.43	.0006	.0005	.0005	.0000
Cl + CH4	.0283	-.0163	0.32	-.0032	-.0052	-.0032	-.0007
O2 + hv	.4696	.0041	0.20	.0036	.0008	.0092	.0018
O3 + hv	-.2785	-.1020	0.10	-.0050	-.0102	-.0077	-.0018
O3 +hv->O(D)	-.1215	.0327	0.25	.0060	.0082	.0052	.0015
O3 P-L	.0537	.0220					

* reaction included in 2-D model error runs

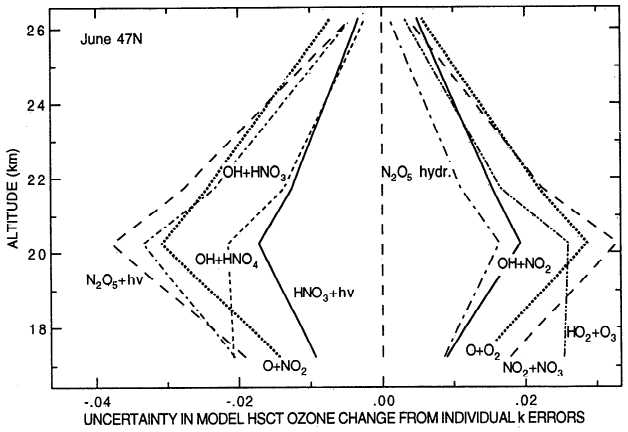

Figure 1. Uncertainty in model ozone change (Table 1 col. 4-7) from HSCT emissions due to 1-σ error rate constant increases in the most sensitive reactions at 47°N vs. altitude.

increasing the rate constants for OH + HNO_3 and HNO_4, reactions reactivating NOx and destroying HOx that have complex pressure and temperature dependent mechanisms with large low temperature error bars. Substantial sensitivities to chlorine chemistry, which interferes with the ability of the added NOx to destroy O_3, are apparent in Table 1, but lower error bars for these reactions reduce their uncertainty contributions at 47°N.

The prominent sensitivity to NO_3 photolysis in Table 1 appears surprising, because photolysis is the nearly exclusive daytime NO_3 loss process, which is already fast, and the daytime NO_3-driven catalytic ozone loss is effectively saturated. It arises from applying Senkin to a diurnally averaged (d.a.) model, for tractable execution times. Senkin computes the sensitivity to the d.a. $J(NO_3)$=ßJ(JPL) from the LLNL model, but holds the d.a. coefficient ß fixed. ß (~.05) couples the 24 hour average abundance of NO_3 (almost solely a function of its night time abundance) to the proper J(JPL) rate for photolysis (which drives O_3 loss); a concentration-weighted average of diurnally-varying J's is made. In the special case of NO_3, changing J(JPL) should produce an inversely proportional change in ß, which effectively compensates for the photolysis frequency change, and leaves the d.a. photolysis rate unchanged as expected. By not allowing this compensation in Senkin, the photolysis change maladjusts the NO_3 average abundance and affects related NOx catalytic O_3 loss chemistry. ß values for N_2O_5 and other species reflect largely the diurnal variation of the radiation field(ß~0.3), remain constant, and hence do not influence O_3 sensitivity.

The NO_2 product channel from NO_3 photolysis does not destroy odd oxygen, in contrast to the NO channel. Treating the two in a decoupled manner elicits a response in O_3 from both channels for the implicitly changed branching ratio. A change in the total photolysis rate constant, without a concomitant change in branching ratio, would produce no response. Direct application in the LLNL 2D model verified this sensitivity behavior for the branching ratio and total photolysis rate. Any uncertainty for this branching ratio (not given in the JPL evaluation) contributes to the overall kinetic uncertainty, and any error in J(JPL) is compensated by a reciprocal change in ß. As a result, the calculated Table 1 sensitivity is a combination of the sensitivity to the branching ratio and of the diurnally averaged Senkin procedure (about 90%), and is appropriately excluded from the uncertainty analysis.

This local sensitivity analysis, incorporating all local photochemical feedbacks, isolates the key reactions determining O_3 losses at peak HSCT injections. Nitrogen species kinetics and photolysis account for 2/3 of this net uncertainty. The uncertainties decline away from the altitude of peak NOx injection (which is also the altitude of sizable NOx interaction and cancellation with the ClOx and HOx chemistry), especially higher up, but the same reactions are involved. Improved determinations of the reaction rates highlighted in Fig.1, or observations sensitive to these same reactions, can reduce contributions of kinetic uncertainties to the model predictions.

The square root of the sum of the uncertainty factors squared (excluding NO_3 photolysis) gives a 0-D analysis kinetics uncertainty in the model prediction for HSCT effects on O_3. This 2-9% uncertainty, on line 7 in Table 2, greatly exceeds the predicted O_3 depletion levels of 1-2%. Since the local analysis neglects transport effects from other latitudes, altitudes, and seasons, we expect the real uncertainty to be lower than the current box model, which isolates the most perturbed regime.

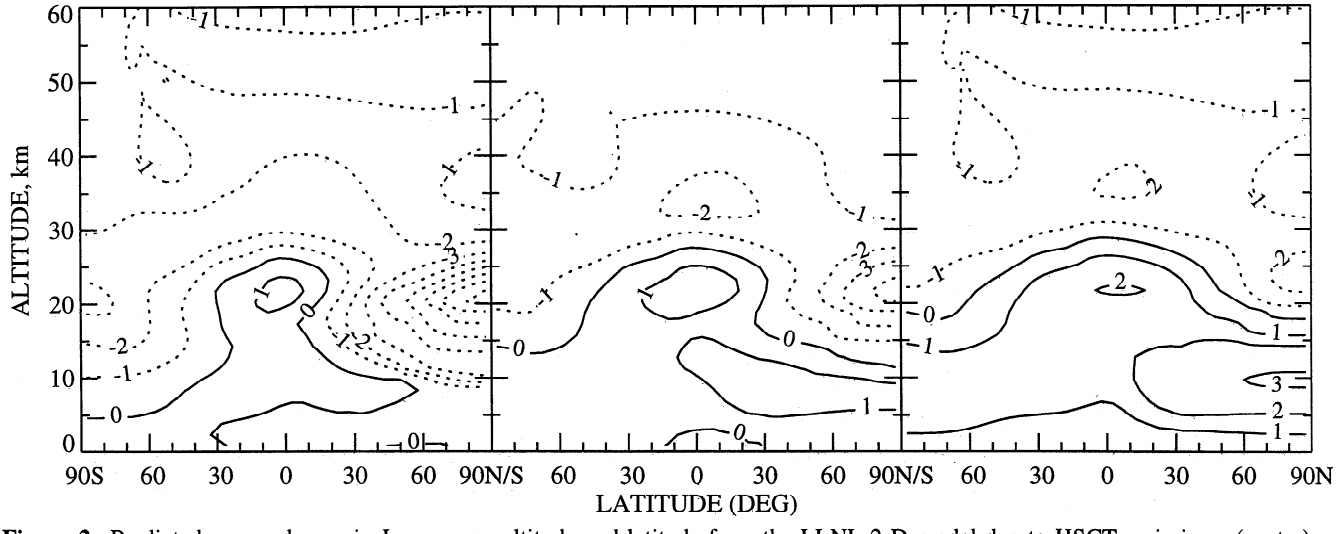

Figure 2. Predicted ozone change in June versus altitude and latitude from the LLNL 2-D model due to HSCT emissions: (center) base case SCN4-SCN0; (first panel) error range run with 9 altered rate constants, maximum depletion; (last panel) error range run, minimum depletion. Dashed lines indicate depletion, at 1% contours.

Thus we next use guided 2-D model results to quantify global uncertainties and estimate scaling factors for the 0-D results.

Sensitivity Guided 2-D Model Runs

Guided by our local results we repeated the 2-D model SCN4 and SCN0 calculations with 9 of the most sensitive perturbation rate constants altered by $1/\sqrt{9}$ of their 1-σ JPL error limits. Reactions starred(*) in Table 1 were altered as a group, using the signs of the sensitivities, in two sets that either maximize and minimize O_3 depletion. Using these input parameter changes we effectively determine the approximate range of HSCT induced O_3 changes due to photochemical uncertainties in the 2-D calculations. The 1/3-σ error sampling runs are roughly equivalent to 80% of the 1-σ rms 0-D uncertainty.

The 2-D June results are shown in Fig. 2 and compared with our 0-D estimates at 47°N in Table 2, the ±k error sampling runs of lines 3-5. Line 6 gives the ratios of the 2-D model variations to those predicted by the box model sensitivity analysis. The 0-D method overstates uncertainty by 20-70%, doing poorest as expected at altitudes of maximum NOx emission. Similar damping factors were seen when only k for $O+NO_2$ was increased(by 20%). Transport and seasonality in the 2-D model couple the 47°N June 0-D boxes to other regions with lower NOx perturbations. A non-linearity is also apparent. If we apply the same empirical damping factors (line 6) to the full 0-D uncertainty analysis (line 7), the final line 8 uncertainties should provide a nonrigorous suggestion of the kinetic reliability of the assessment computations at 47°N. These errors are on the order of 3% O_3 change at a spot of sizable aircraft perturbation, consistent with a kinetics only Monte Carlo error analysis of the NASA-Goddard 2-D model(Stolarski et al., 1995). Altering the HO_2+O_3 rate constant in their model had a much larger effect on O_3 loss than the HO_2+NO rate constant(Considine et al., 1995). Our sensitivities agree in both sign and magnitude. A 3% photochemical uncertainty in predicted local O_3 depletion for the 2-D LLNL model is comparable to the intermodel variability (Fig.24 in Stolarski et al., 1995).

Our sensitivity-guided 2-D kinetic error range calculations on the global O_3 perturbation shown in Fig. 2 also sample photochemistry uncertainty effects at other locations and seasons. The calculated range increases in the lower stratosphere(22km) at high northern latitudes with 1-7% O_3 losses at 62°N June. The calculated column O_3 changes range between -4% and 0% at 62°N, -3% to +0.2% at 47°N, and -2% to 0% at 25°N, with only small seasonal variations(±0.2%). The kinetics only Monte Carlo uncertainties from Stolarski et al.(1995) are about 40% lower. Uncertainties in the southern hemisphere, tropical regions, and high altitudes are small. As rows 3 and 7 in Table 2 show, reaction uncertainties other than the 9 considered likely increase the uncertainty in O_3 perturbation to 1.25 times these values. Additional high latitude uncertainties from halogen and PSC chemistry are likely (Stolarski et al., 1995).

Table 2. Comparison of Ozone Perturbation Uncertainties

1	Altitude (km)	17.25	20.25	21.75	26.25
2	2-D model ΔO3 from HSCT	-.0078	-.0143	-.0151	-.013
3	0-D prediction for the ±k runs	.047	.081	.057	.011
4	2-D +k run effect on HSCT O3	-.037	-.045	-.041	-.023
5	2-D -k run effect on HSCT O3	+.013	+.006	+.001	-.006
6	2-D/0-D model effect ratio	.62/.44	.38/.25	.45/.27	.91/.64
7	0-D HSCT O3 1-σ Uncertainty	.061	.093	.068	.015
8	Estimated 2-D HSCT O3 1-σ Uncertainty	-.038 +.027	-.035 +.023	-.031 +.018	-.014 +.010

Conclusions

We have applied a local sensitivity-uncertainty analysis to a 2-D model assessment of aircraft-induced O_3 depletion in June at 47°N. Photochemical reactions that dominate the uncertainty were identified, and involve aspects of the nitrogen chemistry and its coupling to odd hydrogen. Nine key input rates were altered to chosen limits and 2-D model runs repeated. This limited sampling of photochemical uncertainty space indicates predicted O_3 effects by aircraft are kinetically accurate locally to about 3%. This uncertainty is about twice the size of model predictions themselves and comparable to other uncertainties reflected in intermodel variability, but still provides a reasonable margin for assessment purposes. The 0-D sensitivity analysis isolates key sources of error to guide model refinements, although it overestimates the uncertainty.

Acknowledgments. This work was supported by the Atmospheric Chemistry Program of the U.S. Dept. of Energy(at SRI), the N.S.F. Research Experiences for Undergraduates program.(W.S.H.) and the U.S. Dept. of Energy under Contract W-7405-Eng-48 (at LLNL). We thank the editor and reviewers for valuable comments.

References

Considine, D.B., A.R. Douglass, and C.H. Jackman, Sensitivity of Two-Dimensional Model Predictions of Ozone Response to Stratospheric Aircraft: an Update, *J. Geophys. Res.* 100, 3075-3090 (1995).

DeMore, W. M., S. P. Stander, D. M. Golden, R. F. Hampson, M. J. Kurylo, C. J. Howard, A. R. Ravishankara, C. E. Kolb, and M. J. Molina. Chemical Kinetics and Photochemical Data for Use in Stratospheric Modeling. Jet Propulsion Laboratory, 1994. JPL 94-26.

Johnston, H., Reduction of Stratospheric Ozone by Nitrogen Oxide Catalysts from Supersonic Transport Exhaust, *Science* 173, 517-522 (1971).

Lutz, A. E., R. J. Kee, and J. A. Miller. SENKIN: A Fortran Program for Predicting Homogeneous Gas Phase Chemical Kinetics with Sensitivity Analysis. Sandia National Laboratories, 1988. SAND87-8248-UC-4.

Stolarski, R.S., S.L. Baughcum, W.H. Brune, A.R. Douglass, D.W. Fahey, R.R. Friedl, S.C. Liu, R.A. Plumb, L.R. Poole, H.L. Wesoky, and D.R. Worsnop, 1995 Scientific Assessment of the Atmospheric Effects of Stratospheric Aircraft, NASA Ref. Publ. 1381, 1995.

World Meterological Organization, Scientific Assessment of Ozone Depletion 1994, WMO Report 37, Chapter 11, 1994.

Wuebbles, D., P. Connell, K. Grant, D. Kinnison, and D. Rotman. "LLNL Two-dimensional Chemical-Radiative-Transport Model." In The Atmospheric Effects of Stratospheric Aircraft: Report of the 1992 Models and Measurements Workshop, NASA Ref. Pub. 1292, 1993.

M. K. Dubey, MS J585, CST-6, Los Alamos National Laboratory, Los Alamos NM 87545. Email : dubey@lanl.gov

G. P. Smith, SRI International PS-047, Menlo Park CA 94025. Email: smith@mplvax.sri.com

W. S. Hartley, Atmospheric Sciences Dept., University of Washington, Seattle WA 98195

D. E. Kinnison and P.S. Connell, Lawrence Livermore National Laboratoty, Livermore CA 94550. Email: kinnison1@llnl.gov, connell2@llnl.gov

(Received: April 15, 1997; revised: September 22, 1997; accepted: October 6, 1997)